

Engineering Safe Shear Dilatancy for the Development of EGS Reservoirs

François H. Cornet

EOST, 5 rue René Descartes, 67080, Strasbourg, France

Francois.cornet@unistra.fr

Keywords: hydraulic fracturing, shear induced dilatancy, Representative Elementary Volume (REV), effective stress failure criterion, quasi-static shear motion.

ABSTRACT

The classical hydraulic stimulation technology as applied to the development of oil and gas reservoirs implies the injection of proppant in hydraulic fractures in order to keep the fractures opened when injection stops. An alternative technology that relies on shear induced dilatancy and does not require the injection of proppant has also been proposed for the development of high temperature Enhanced Geothermal Systems (EGS).

Both techniques have been tested in the shallow depth (750 m) of the granitic rock mass at le Mayet de Montagne (France). Only the shear induced dilatancy has revealed to be efficient in this formation because channeling effects were found to limit the size of hydraulic fractures. The interconnectivity of these channels has been found to result in a very heterogeneous pore pressure field at the scale of the reservoir, with consequences for the definition of the Representative Elementary Volumes (REV) to be considered for the definition of effective stresses. Then, the efficiency of shear induced dilatancy has been tested successfully for the development of two EGS reservoirs at Soultz-sous-forêts (France), the first one within a 2850 m - 3400 m depth range, the second one within a 4500 m – 5000 m depth range.-.

After analyzing these results, we propose a method for designing shear induced dilatancy in hot but impervious geothermal reservoirs. Once the complete regional stress field has been properly assessed, the development of fresh shear zones may be designed by direct application of the Terzaghi effective stress concept, when considering Representative Elementary Volumes (REV) with size in the order of $30 \times 30 \times 30 \text{ m}^3$ together with the Hoek and Brown failure criterion.

But shear stimulations generate micro seismic events, the magnitude of which may not be compatible with the surface use of land. Interestingly, results from Soultz outline the existence of large scale non-seismic shear motions. We propose to take advantage of these aseismic slips and to apply the concept of fatigue through cyclic variations of effective stresses in volumes larger than that of the REV for keeping the magnitude of micro-seismic activity to acceptable levels.

1. INTRODUCTION

In the mid-eighties, a shallow test site in granite was developed for investigating in situ the effectiveness of various hydraulic simulation techniques for the development of what was known then as Hot Dry Rock geothermal systems (e.g. Cornet, 1989). Both hydraulic fracturing with proppant and shear induced dilatancy were investigated. Results suggested that only shear induced dilatancy was promising and the method was applied then at the European experimental geothermal site of Soultz-sous-forêts, in Eastern France. On the Soultz site, where temperature reaches 200°C at 5 km, two reservoirs have been developed, the first one within the 2800 m to 3500 m depth range and the second one within the 4500 m to 5 Km depth range (e.g. Genter et al., 2010). The development of both reservoirs relied strongly on shear induced dilatancy, although the deeper reservoir has also benefitted from chemical leaching (Portier et al., 2009).

After a presentation of results obtained at both sites, we concentrate in this presentation on hydro-mechanical aspects of hydraulic stimulations through shear induced dilatancy in order to outline a simple design methodology. Finally we propose a new stimulation technique in order to keep induced seismicity at acceptable levels.

2. HYDRAULIC STIMULATIONS AT THE LE MAYET DE MONTAGNE TEST SITE (CENTRAL FRANCE)

From 1978 to 1987, in situ experiments on hydraulic stimulations were conducted in two 800 m deep boreholes (INAG III-8 and INAG III-9), 100 m apart, that had been percussion drilled in the granite massif of le Mayet de Montagne (central France). The objective was to develop a water circulation between both wells within the 600m - 820m depth range.

The depth interval was chosen so as to be free of topographical effects, which revealed to be noticeable down to 400m (e.g. Cornet and Yin, 1995), but shallow enough for providing the possibility of installing a wealth of observation stations: 15 three-components seismometers for the monitoring of induced seismicity (Talebi and Cornet, 1987), and six stations for ground motion measurements.

First we recall some results from the hydraulic fracturing stimulations. Then we show how micro-seismic observations collected during the shear induced dilatancy experiments together with direct stress measurements, help to map the pore pressure in the reservoir.

2.1 On the Lateral Extension of Hydraulic Fractures in a shallow granite massif.

Ground surface deformations were monitored throughout the program with an array of 5, temporarily 6, tilt stations (Cornet and Desroches, 1990). One of the stations was located in between the wellheads, 64 m to the north of INAG III-9. The other stations were distributed around the wells at distances ranging from 120 to 300 m. Each station included two silica-based tilt meters set in two orthogonal directions, with one of them pointing roughly toward INAG III-8 well head. In addition, at each station, a temperature sensor monitored continuously the temperature some 5 cm below ground surface. Resolution of the tilt meters was better than $5 \cdot 10^{-8}$ radians, as demonstrated by the clear recording of earth tides.

A first set of hydraulic stimulations was conducted in INAG III-9, during which gel was injected through a straddle packer in four preexisting fractures located at various depths below 600 m. It was followed up by a true hydraulic fracture operation conducted at the bottom of well INAG III-8, during which 200 m³ of high viscosity gel and 40 tons of sand were injected with a 4.4 m³/min flow rate.

For none of these various stimulations was any tilt larger than $5 \cdot 10^{-7}$ radian recorded. An elastic analysis of this lack of surface tilt (Desroches and Cornet, 1990) showed that for none of the stimulations did the mechanically open part of the stimulated fractures reach a radial distance from the well larger than 50 m. It was concluded that flow at larger distances from the well occurred through local interconnected channels imbedded in the natural fault and fracture system.

Hence attention turned to better understanding the flow pattern in the natural fault and fracture system and a new method for mapping the pore pressure away from the wells was developed.

2.2 Mapping the Pore Pressure during the Stimulation and Circulation Experiments at Le Mayet de Montagne.

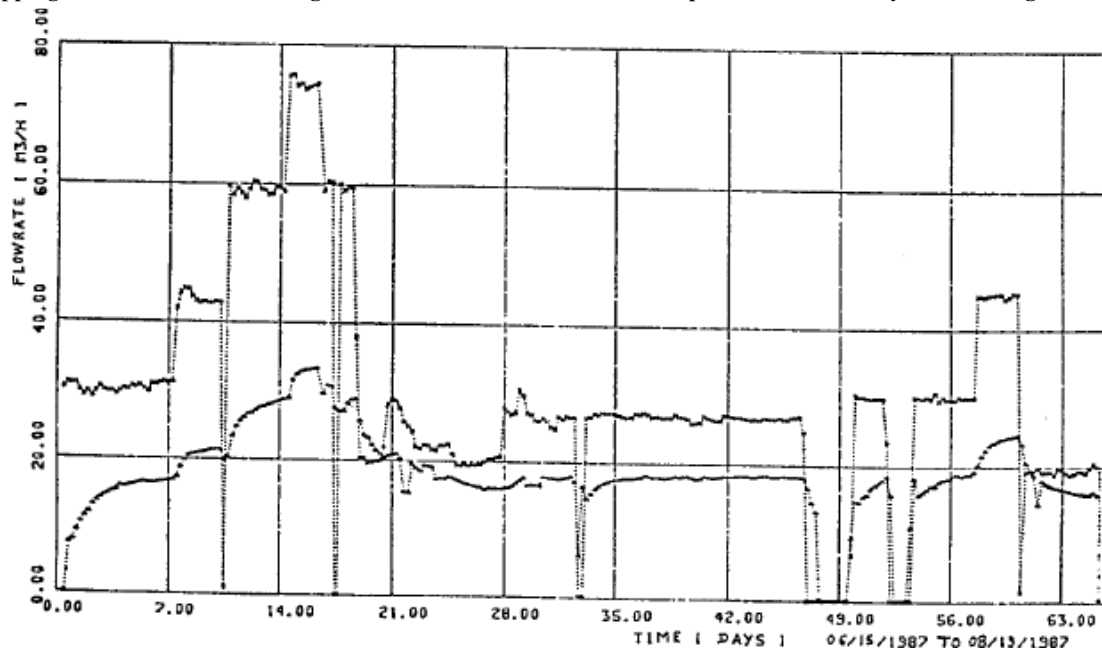


Figure 1: Well head injection flow rate and well head production flowrate observed during the hydraulic stimulation and the long term circulation experiment at Le Mayet de Montagne (after Cornet, 1989).

The initial site reconnaissance program was designed to produce a sound understanding of the hydraulic characteristics of the regional fracture pattern as well as a precise knowledge of the regional stress field thanks to numerous hydraulic tests. Then, after the stimulation program has been completed, a long term (66 days) circulation experiment was undertaken with injection at various flow rates in the open hole section of well INAG III-9 below 600 m (figure 1). During both the stimulation and the circulation periods induced seismicity was continuously monitored with a network of 15 three components stations with linear response in the 10 - 2000 Hz frequency range, and located in the granite at the bottom of boreholes with depths ranging from 20 to 150 m.

All together 107 micro-seismic events were recorded during the various stimulation and circulation phases and their location is shown on figure 2. On this figure events within the red contour occurred at depths smaller than 600 m, i.e. at depths above the injection domain, whilst those within the green contour occurred within one of the zones that had been hydraulically stimulated.

After the focal mechanisms for all these events have been determined, Yin and Cornet (1994) integrated them with the results from hydraulic stress measurements (measurement of normal stress supported by fracture planes with known orientation) in order to obtain a well constrained regional stress field characterization. The solution was found to be homogeneous with 95 % of the hydraulic stress measurements and 70 % of the focal plane solutions. This comes in support with the conclusion derived from the absence of tilts that flow occurred along channels within the natural fracture network: locally, along a given channel, the stress may be different from the mean regional stress defined at a larger scale. But the fact that 70 % of the focal mechanisms are homogeneous with this mean stress field demonstrates that the sources for stress heterogeneity are only local and do not prevent the

definition of a uniform mean stress within volumes, the size of which is defined by that of micro-seismic events. Given most of the magnitudes for these events are smaller than 1 and therefore exhibit sizes smaller than 30 m, it may be concluded that, for this site, the size of the Representative Elementary Volume (REV) is of the same order of magnitude as that of these events, i.e 30x30x30 m³.

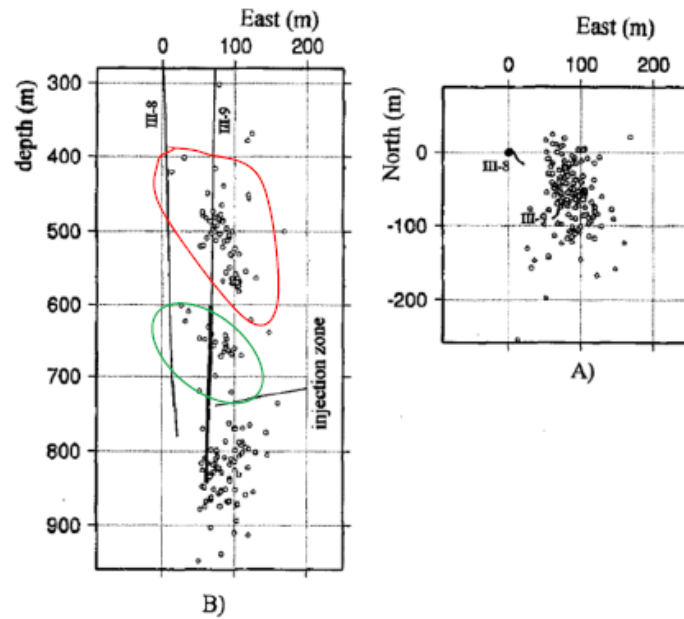


Figure 2: Location of micro-seismic events observed during the hydraulic stimulation and long term circulation experiment (after Cornet and Yin, 1995).

Cornet and Yin (1995) have taken advantage of all the focal mechanisms that are homogeneous with the computed mean stress field for identifying the local pore pressure that induced these events. They assume that an unstable slip occurs when the resolved shear stress τ supported by a given fracture plane satisfies the Coulomb failure criterion expressed in terms of effective stresses. Further, neglecting the cohesive strength of the fracture, they propose that slip occurs when

$$\tau = \mu [\sigma_n - \beta (P_0 + dP)] \quad (1)$$

where μ is the friction coefficient for the fracture surface, σ_n is the normal stress component supported by the fracture plane, P_0 is the original hydrostatic pore pressure at the event location, dP is the pore pressure perturbation caused by injection, and β is a coefficient that takes into account the effective stress concept.

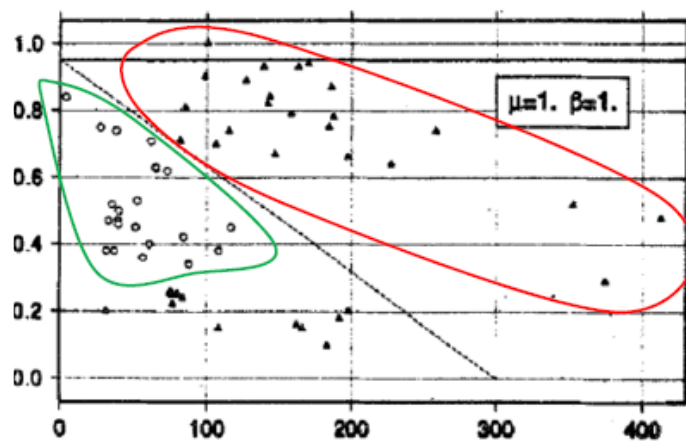


Figure 3: Mapping of the pore pressure perturbation generated by the water injection (after Cornet and Yin, 1995). The horizontal axis is the distance to the injection well and the vertical axis is the ratio between the pore pressure perturbation at the even location and the pressure at the same depth in the well (dP/P_i).

But the pore pressure perturbation cannot be larger than the pressure in the injection well, P_i , at the depth of the event, and cannot be negative. Hence they looked at the set of values for parameters μ and β which satisfy the pore pressure perturbation condition $0 \leq dP/P_i \leq 1$.

They investigated all the combination of values 0.5, 0.6, 0.7, 0.8, 0.9, 1, 1.1, 1.2 for the friction coefficient and 0.8, 0.9 and 1 for parameter β . Interestingly, for β values smaller than 1, they noted that some of the events would have required a pressure

perturbation larger than the pressure in the injection well, whatever the value considered for the friction coefficient. Hence they set $\beta = 1$ in equation (1), which corresponds to Terzaghi effective stress concept. Then, only the friction coefficient with values between 0.6 and 1 were found to be compatible with the pore pressure perturbation condition as expressed here above.

Results shown on figure 3 correspond to a value of 1 for the friction coefficient. The possibility of such a high value for μ is likely caused by the assumption of zero cohesion for all fractures. It may be noted on figure 3 that, for all the events located within the red contour, the pore pressure remains very high although the distance to the well reaches more than 200 m. But, for events within the green contour, the pore pressure is found to drop as the distance to the well increases. This implies that flow rate through the channels that connect the injection well to all the events located within the red contour is very small, if not null. Further, the pressure drop observed for the events located within the green contour may be used to evaluate the hydraulic conductivity in the corresponding fracture network.

Interestingly, figure 2A shows that no micro-seismic event was observed in the vicinity of the production well III-8, even though some very significant flow was measured in this well, as shown on figure 1. This is because the pore pressure in the vicinity of the production well is close to hydrostatic pressure and is too small for satisfying equation (1). This demonstrates that micro seismicity induced by forced fluid injections outlines zones of high pore pressure perturbation, and **NOT** zones of high flow rate.

2.3 Dimensions of the REV for Absolute Stresses and for Effective Stresses for the Le Mayet de Montagne Test Site.

Figure 3 shows that the pore pressure within the granite rock mass, where induced seismicity has been observed, is very heterogeneous. For channels where water is flowing, the pressure drops regularly as the distance to the injection well increases. However, some channels have been found to be connected hydraulically to the injection well but not connected to any far-field flowing zone, so that pore pressure is high in these channels because of the absence of flow.

Validity of this proposition was demonstrated by injection tests conducted after the injection well INAG III-9 had been cleared of all the completion required by the long term circulation. Cornet and Morin (1997) conducted injection experiments in an open-hole section of INAG III-9 extending from 250 m down to the bottom of the well. For various injection flow rates, they conducted flow logs in order to determine flow losses through the various fracture systems connected to the well. They observed that no flow was lost in the 450 – 550 m depth range where micro-seismic activity had been detected during the previous experiments, for injection pressures smaller than the local minimum principal stress magnitude. But when the injection pressure became large enough a preexisting fracture was opened that took up most of the flow.

We conclude here that, whilst the minimum size of the REV to be considered for the definition of “mean” absolute stresses in this rock mass is larger than 30x30x30 m, the REV used for the definition of *effective* stresses is much smaller and is controlled by the pore pressure gradients in the fracture system. These pressure gradients depend on both the injection pressure and the minimum principal stress magnitude. A clearer picture of the influence of the minimum principal stress magnitude for the definition of the size of the REV for effective stresses is provided by results from hydraulic stimulations conducted at greater depth, as shown by results obtained at the Soultz-sous-forêts site discussed here after.

3. HYDRAULIC STIMULATIONS IN A GRANITIC ROCK MASS AT DEPTHS GREATER THAN 2500 M

In the early nineties, a consortium between France, Germany and the UK, with a support from the European Economic Community, selected the buried granite massif at Soultz-sous-forêts in north-eastern France, for developing an in situ experimental geothermal site. The objective was to research possibilities of extracting economically the heat from this deep impervious crystalline formation (Gerard et al, 2006; Genter et al., 2010; Schill et al., 2017).

Between 1991 and 1997, a first reservoir was developed at depths ranging from 2800 m to 3600 m, between two wells (GPK1 and GPK2) distant from each other by about 450 m and reaching a temperature of 160°C. Then from 1998 to 2010 a deeper reservoir was developed within the 4500 m – 5000 m depth range where temperature reaches 200°C. It involved the deepening of well GPK2 and the drilling of two deviated wells, GPK3 and GPK4, such that the bottom-hole distance between GPK2 and GPK3 is 650m and that between GPK3 and GPK4 is 700m.

Both reservoir developments involved hydraulic stimulations based on the concept of shear induced dilatancy but no hydraulic fracturing operation with proppant has been undertaken. The various hydraulic stimulations were monitored with both a surface and a downhole seismic network. The downhole network involved 4 components stations, with resonance free response from a few Hz to over 1 KHz. They were set at the bottom of wells reaching the top of the granite at depths close to 1500 m (Jones et al., 1997).

3.1 The Three Levels of Non-Linear Hydro-Mechanical Coupling Observed at Soultz-Sous-forêts

The main hydraulic stimulation undertaken for developing the upper reservoir involved a multistep injection experiment as shown on figure 4. Injection proceeded in two phases. First, the well was sanded in, up to 3400 m, in order to avoid stimulating a large fault intersected around 3490 m. Then the sand was washed out and injection took place along the complete open-hole section. During the first phase, injection proceeded for 16 days with a stepped incremental flow rate ranging from 1 l/sec to 36 l/sec. Once injection rate reached 6 l/sec, each step lasted 48 hours with flow rate increments equal to 6 l/sec from one step to the next. The total injected volume reached 25 300 m³. During the second phase that lasted about 5 days, injection started at 41 l/sec and was later increased to 50 l/sec for a total injected volume equal to 19 300 m³.

During the first phase, the well-head injection pressure rose progressively with each flow rate increment. But once the flow rate reached 18 l/sec, it stabilized so that the borehole pressure increment at 2850 m was 9.1 MPa (10 MPa well-head pressure). Spinner logs were run every 24 h for monitoring flow rate profiles in the well (Cornet and Jones, 1994; Evans et al., 2005). They showed that, below a 10 MPa well-head pressure, each flow rate increment, and therefore each pressure increment, resulted in proportionately more flow reaching the deeper parts of the well. But once the pressure stabilized, the increment in flow rates

resulted only in proportionately more flow leaving the upper portion of the well. The stabilization of injection pressure despite the increase in injection flow rate suggests that fractures were opening in the upper part of the well. However it must be outlined that no real large scale hydraulic fracture was subsequently observed in the well during the ultrasonic borehole imaging log.

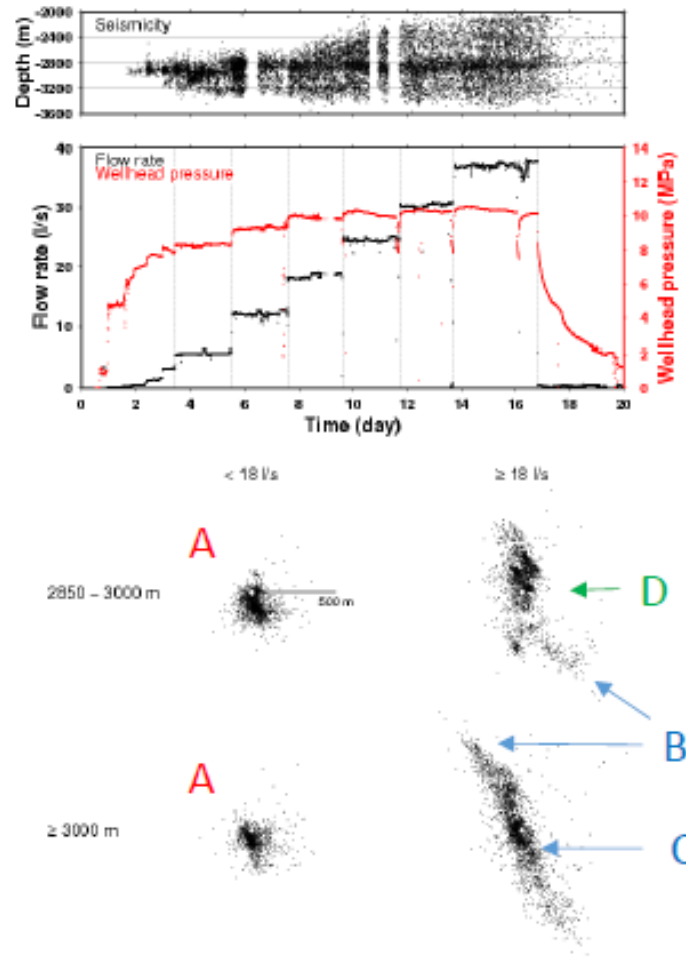


Figure 4: The first phase hydraulic stimulation and the location of induced micro-seismic events (after Cornet et al., 2007). Letter A indicates events that correspond to linear poro-elasticity whilst letters B, C and D indicates events that correspond to non-linear hydro-mechanical coupling. The upper graph illustrates the vertical growth of the seismic cloud as injection proceeded.

The upper plate in figure 4 illustrates the depth of micro-seismic events detected with the downhole seismic network. It may be observed that some activity starts close to the casing shoe, when the well head pressure gets larger than 5 MPa and then the seismic cloud extends downward with time, as the well-head pressure keeps increasing. Simultaneously to the downward growth, a small upward growth is observed till day four of injection, when the upward growth stops till day 8. After day 8, the seismic cloud starts propagating upward, when the injection pressure stabilizes although the injection flow rate keeps increasing. Furthermore no significant downward growth is observed any more.

The lateral growth of the seismic cloud as observed for different depth ranges (lower plate of figure 4) has been previously discussed (e.g. Cornet, 2016). It may be noticed that, for injection flow rates smaller than 18 l/s, the growth of the seismic cloud remains axisymmetric, whatever the depth, and corresponds to the linear poro-elastic response of the rock mass. For larger injection flow rates, the orientation of the seismic cloud varies with depth because the hydro-mechanical coupling becomes non-linear. It involves some shear induced dilatancy associated either with the percolation through preexisting structures (letters B) or through the creation of a fresh shear zone (letter C), the orientation of which depends on the minimum principal stress magnitude, and therefore on depth. It was initially proposed that the non-linear hydro-mechanical coupling associated with the upward growth of the seismic cloud was associated with the development of a fresh hydraulic fracture (letter D).

But recently, Cornet (2019) noticed that the injection pressure for which an upward growth of the seismic cloud is observed corresponds precisely to the magnitude of the minimum principal stress at 2900 m, as determined by Cornet et al. (2007). Hence he concludes that, at that depth, the effective minimum principal stress is zero if the pore pressure drop in the immediate vicinity of the well remains negligible. This would imply that preexisting fractures preferentially oriented nearly perpendicularly to the minimum principal stress direction open up and extend upward. This mechanism is consistent with the absence of a clear hydraulic fracture as shown by the acoustic tele-viewer log run just after the stimulation and is similar to the failure process observed for uniaxial compression tests conducted in the lab (e.g. Jaeger and Cook, 1979, chapt. 6).

3.2 The REV Size for Effective Stresses at Soultz and the Hoek and Brown Failure Criterion

The purpose of the multistep flow rate injection process was to build up progressively the pore pressure in the natural fracture system. Given the low hydraulic conductivity of the rock mass (smaller than 10^{-16} m² according to Shapiro et al., 1999), it may be proposed that when the injection pressure stabilized, the borehole pressure value at the base of the casing was very close to that of the pore pressure in the immediate vicinity of the well.

The magnitude of most seismic events varies between 0 and 1.5 so that the size of the events is somewhere between 10 and 70 m, which we take as the size of the REV for this rock-mass (say 50x50x50 m³). But the seismic cloud outlines clearly two different kinds of percolation process: mechanism B corresponds to flow along preexisting planar structures, whilst the seismic cloud associated with mechanism C outlines a ribbon-like vertical continuous structure, the horizontal cross-section of which rotates with depth (lower plate of fig. 4). It has been interpreted as a fresh shear zone that developed within a domain that exhibits increasing effective minimum principal stress with depth. According to stress measurements (Cornet et al., 2007), the effective minimum principal stress component is zero at the top of the open-hole section but increases progressively down to 3500 m.

Assuming that the Hoek and Brown compressive failure criterion (1980) may be used for characterizing this failure process, the in situ stress measurements may be taken to advantage for determining parameters m and σ^c of this criterion. Considering Terzaghi effective stresses, the Hoek and Brown criterion may be written

$$\sigma_1' = \sigma_3' + \sigma^c [m (\sigma_3' / \sigma^c) + 1]^{1/2} \quad (2)$$

We note that, as a first approximation, this criterion does not depend on the intermediate principal stress. Hence, given the in situ stress field variation (in MPa/m) with depth z (in meters) is characterized by

$$\sigma_v = 33.8 + 0.0255 (z - 1377) \quad (3a)$$

$$\sigma_h = 0.537 \sigma_v \quad (3b)$$

$$0.95 \sigma_v \leq \sigma_H \leq 1.1 \sigma_v \quad (3c)$$

we get $36 \leq \sigma^c \leq 42$ and $5 \leq m \leq 11$.

The values identified for parameter m are in the range of those identified by Hoek and Brown for carbonates, mudstone or shale, i.e. for the type of material expected to be encountered in the filling of faults and large fractures, but not that of the homogeneous granite as determined by Vileneuve et al. (2018). This suggests that the “compressive strength” characteristics of the equivalent homogeneous material that fills up the REV is mostly dependent on the characteristics of the fracture network and its filling material rather than on the properties of the fresh granite.

After a 4 months long circulation experiment was conducted between GPK1 and GPK2, the decision was taken to develop a deeper reservoir at 5 km, for temperatures in the range of 200°C (Gerard et al., 2006). The GPK2 well was deepened and the two deviated wells, GPK3 and GPK4 were drilled so that they remain in a vertical plane oriented parallel to the maximum horizontal principal stress direction. The well GPK3 was found to intersect a major fault zone with a vertical extension up to the upper reservoir, but the well GPK2 was found to intersect a sound granite and was hydraulically stimulated following a stepped injection rate procedure (e.g. Calo et al., 2011). The stimulation of well GPK4 involved mostly chemical leaching (Genter et al., 2010). We discuss here after results from the GPK2 stimulation.

3.2 Application to the 5Km Deep GPK2 Well Hydraulic Stimulation

As for the previous stimulations, induced micro-seismicity was monitored with both a surface and downhole networks (Cuenot et al., 2007). The downhole network involved the same stations as for the 1993 GPK1 stimulation plus an additional station in a well reaching also the top of the granite. The surface network included all together 18 stations. A temporary network was deployed, which included 8 stations with a single vertical component and 5 stations with three components. It was complemented with an additional 3 three-components stations from the permanent regional seismic monitoring network and a broad-band station (Calo et al., 2011).

Incompressible fluids were injected with a rate at 30 l/sec for 24 h, followed by a 40 l/sec flow rate for 27 h and finally a 50 l/sec flow rate for another 90 h (upper plate in figure 5). Total injected volume reached 23 400 m³, i.e. a value somewhat similar to that of the 1993 GPK1 stimulation.

Some seismic activity was detected nearly immediately after injection has started and stopped after injection stopped. The development of the seismic cloud with time is illustrated by the lower plate of figure 5. As long as injection is on-going, the volume within which events are observed remains fairly well constrained and is somewhat similar in shape to that observed during the shallower reservoir development in the 3 km depth range. But when injection stops, percolation occurs through the natural fractures and faults system, away from the initial seismic cloud. Interestingly, the largest magnitude (2.6) was observed after injection has stopped (Cuenot et al., 2007).

Results from seismic tomography have led Calo et al. (2011) to propose that a large scale non-seismic shear motion occurred within the cloud when injection rate changed from 30 l/sec to 40 l/sec. We examine now, how this shear rupture fits with the Hoek and Brown criterion, given the regional stress field is described by equations 3a to 3c.

We have shown that the so-called uniaxial compressive “strength” of the rock mass may be estimated to range from 36 to 42 MPa. We may compute the predicted maximum horizontal principal stress at 4800m, on the assumption that it caused the shear failure of the rock mass when the wellhead pressure reached 12 MPa. For a value of 5 for parameter m in equation 14 and a uniaxial strength

of 36 MPa we get a value of 114 MPa for σ_H and a value of 132 MPa if the parameter m is taken equal to 10 and the uniaxial strength is taken equal to 42 MPa, given the vertical stress at 4800 m is 121 MPa. These results fit very nicely within the interval proposed for the maximum horizontal principal stress magnitude at this depth by the stress measurements, namely (115 MPa - 133 MPa).

We may conclude that the Terzaghi effective stress concept combined with the Hoek and Brown failure criterion helps predict the development of the fresh shear zones created during the various hydraulic stimulations at Soultz.

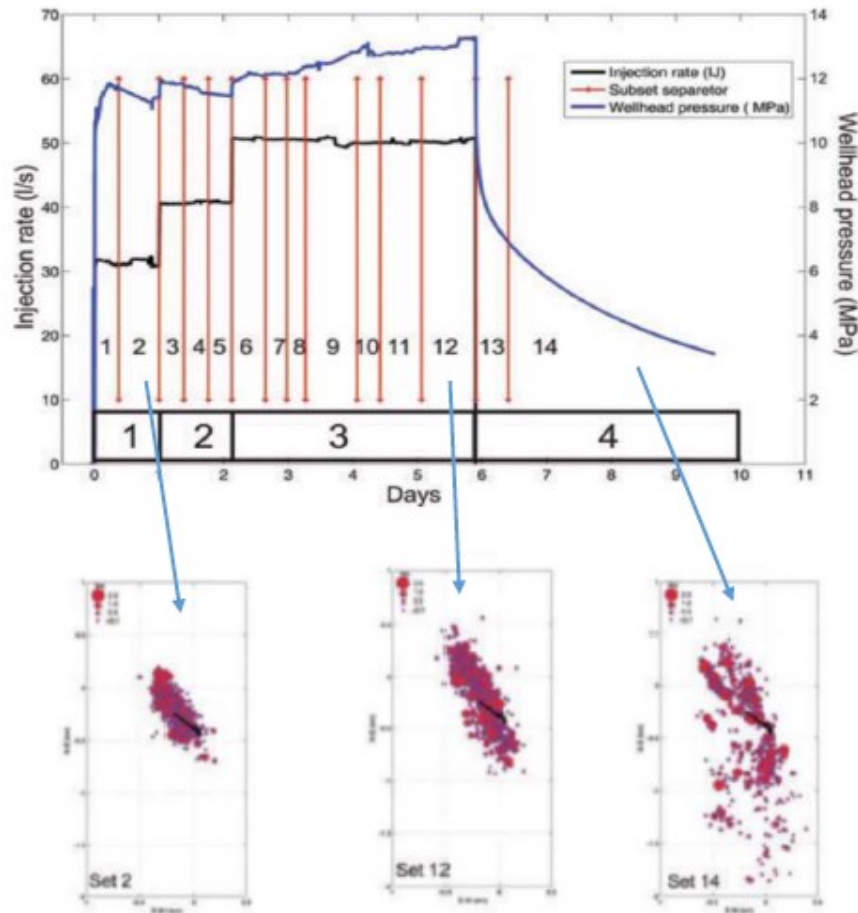


Figure 5: Location of micro-seismic events observed during the 5 km deep hydraulic GPK2 stimulation (after Calo et al., 2011).

4. ELEMENTS FOR THE DESIGN OF SAFE SHEAR INDUCED DILATANCY

An important issue raised by the growth of the seismic cloud during the deep GPK2 stimulation is the change in dynamics of the growth of the micro-seismic cloud: For all the period during which injection is proceeding the cloud remains fairly localized, but once injection stops, and therefore pore pressure drops in the vicinity of the well, the seismic activity extends throughout the fractures and faults network away from the well. Furthermore, the largest micro-seismic event (magnitude 2.6) is observed whilst the pore pressure is dropping in the vicinity of the well.

Similarly, the largest magnitudes observed during the Basel experiment have been observed at the end (magnitude 3.4), and mostly after (magnitudes between 3.1 and 3.2), the stimulation (Häring et al., 2008; Deichmann and Giardini, 2009). But, for this site, the total injected volumes (11 570 m³) is quite smaller than those injected at Soultz during the various hydraulic stimulations. This raises the question whether a different injection protocol for the stimulation in Basel would have resulted in quite smaller magnitudes.

Another important issue raised by the hydraulic stimulations conducted at Soultz is the identification of large aseismic motions (Cornet, 2016). Such aseismic-seismic transitions have been often discussed (e.g. Scholtz, 1990; Guglielmi et al., 2015) and models have been proposed that rely on the dependency of the friction coefficient on slip velocity and the wearing of the slipping surfaces.

Since the mid-seventies it is well recognized that the seismic moment is a more appropriate quantity for characterizing the energy associated with seismic events than their magnitude (e.g. Stein and Wyssession, 2003). The seismic moment M_0 of shear events is

$$M_0 = G U A \quad (4)$$

where G is the elastic shear modulus of the rock, U is the amount of slip, and A is the area of slip. Hence, a decrease of the elastic shear modulus of the rock mass surrounding the slipping surface would reduce the energy associated with the unstable slip.

In the early seventies, Haimson and Kim (1972) investigated the principle of fatigue on rock specimens loaded under uniaxial compression conditions. They observed that repeated load-unload cycles could lower significantly the compressive strength of these samples as well as their elastic Young's modulus.

Hence, we propose here to apply this principle of fatigue to rock masses, by cycling the pore pressure in volumes quite larger than that of the REV. This should decrease progressively the elastic shear modulus of the rock mass, and therefore the elastic energy stored in the vicinity of expected large slip events, and therefore the magnitude of the events.

It may be noted on figure 5 that the shape of the seismic cloud observed during the stimulation of GPK2 outlines a lack of pore pressure variation outside the volume where micro-seismicity is occurring. This suggests that no significant pressure perturbation takes place away from this cloud. As a simple model, the material where micro-seismicity occurs may be considered as an elongated Eshelby soft inclusion. When the pore pressure increases inside this inclusion, it generates tangential compressive stresses at the boundary of the inclusion, which decrease the hydraulic conductivity of the rock mass surrounding the inclusion, and therefore limit the flow away from the inclusion. This is the volume that should be fatigued for preventing large micro-seismic events.

5. CONCLUSIONS

Integrated inversions of focal mechanisms from induced seismicity together with results from hydraulic stress measurements may be taken to advantage for defining the mean stress field in large rock masses. Micro-seismic events that are homogeneous with this mean stress may be used to map the pore pressure field during hydraulic stimulations. When applied to the data obtained at le Mayet de Montagne, this mapping technique has outlined the role of boundary conditions for the flow in the interconnected channel system, as well as that of the difference between the pore pressure and the local minimum principal stress magnitude. The strong pressure gradients within the REV defined for the large scale absolute stress field prevents the definition of Terzaghi effective stresses at the same scale, so that the REV for effective stresses is much smaller with strong consequences for the efficiency of hydraulic stimulations.

But hydraulic stimulations conducted at the greater depths of the geothermal site at Soultz-sous-forêts, have shown that during stimulation the pore pressure remains fairly uniform in large volumes around the well so that the effective stress concept may be applied for REV in the range of $50 \times 50 \times 50 \text{ m}^3$. At this scale, the development of fresh shear failures has been found to be well characterized by the Hoek and Brown failure criterion.

This opens the way to a new hydraulic stimulation procedure that relies on fatigue testing by cycling the pore pressure in order to decrease the amount of energy radiated by induced micro-seismicity.

ACKNOWLEDGEMENT

This presentation has been sponsored by the LABEX G-eau-thermie at EOST (Université de Strasbourg)

REFERENCES

- Calo, M., Dorbath, C., Cornet, F. H., and Cuenot, N.: Large scale aseismic motion identified through 4D P-wave tomography. *Geophys. J. Int.* **186**, (2011), 1295-1314.
- Cornet F.H.: Experimental investigation on forced fluid flow through a granite rock mass; *European Geothermal update* (K. Louwrier et al., ed.), Kluwer academic publishers, (1989) 189-204.
- Cornet, F.H.: Seismic and aseismic motions generated by fluid injections; *Geomech. Ener. Env.*, **5**, (2016), pp 42-54
- Cornet, F.H.: The engineering of safe hydraulic stimulations for EGS development in hot crystalline rock masses; *Geomech. Ener. Env.*, (2019), in press
- Cornet, F. H., Berard, Th. and Bourouis, S.: How close to failure is a natural granite rock mass at 5 km depth. *Int. J. Rock Mech. Min. Sc.*, **44(1)**, (2007),. 47-66.
- Cornet F.H., and Desroches J.: The problem of channeling in Hot Dry Rock Reservoirs; *Hot Dry Rock* (edited by R. Baria), Robertson Scientific Publication, (1990).
- Cornet F.H., and Jones R.: Field evidence on the orientation of forced water flow with respect to the regional principal stress direction; *Rock Mechanics-Models and measurements*; (Nelson and Laubach ed.) Balkema, (1994) pp 61-69.
- Cornet F. H. and Yin, J. M.: Analysis of induced seismicity for stress field determination and pore pressure mapping. *Pure App. Geophys.*, **145**, (1995), 677-700.
- Cornet F.H., and Morin R.: Evaluation of hydromechanical coupling in a granite rock mass from a high volume, high pressure injection experiment: Le Mayet de Montagne, France; *Int. J. Rock Mech. Min. Sc.*, **34(3/4)**, (1997), paper nb 207
- Cuenot N., Dorbath C., and Dorbath L.: Analysis of the micro-seismicity induced by fluid injections at the EGS site of Soultz-sous-forêts (Alsace, France): Implication for the characterization of the geothermal reservoir properties; *Pure App. Geophys.*, **165**, (2007), 797-828.
- Desroches J., and Cornet F.H.: Channeling and stiffness effects on fluid percolation in jointed rocks; *Rock Joints* (Barton and Stephansson, ed), Balkema pub., (1989), 527-534.

- Evans K., Genter A., and Sausse J.: Permeability creation and damage due to massive fluid injections into granite at 3.5 km at Soultz: 1. Borehole observations; *J. Geophys. Res.*, 110, B04303; (2005), doi:10.1029/2004JB003168
- Genter A., Evans K., Cuénot N., Fritsch D., and Sanjuan B.: Contribution of the exploration of deep crystalline fractured reservoir of Soultz to the knowledge of enhanced geothermal systems (EGS), *C.R. Geoscience* **342** (2010), 502-516.
- Gérard A., Genter A., Kohl T., Lutz P., Rose P., and Rummel F.: The deep EGS (Enhanced Geothermal System) project at Soultz-sous-Forêts (Alsace, France) *Geothermics*, **35**(5-6), , (2006), 473-483.
- Guglielmi Y, F. Cappa, J.P. Avouac, P. Henry, D. Elsworth: Seismicity triggered by fluid injection-induced aseismic slip; *Science*, **348**(6240), (2015).pp1224-1226.
- Haimson, B. C., and Kim, C. M.: Mechanical behavior of rock under cyclic fatigue. *Proceeding of 13th symp.on Rock Mech.* (Cording ed), American Soc. Civil Eng. Publication, (1972), pp 845-863
- Hoek, E., and E.T. Brown, *Underground Excavations in Rock*. The Institute of Mining and Metallurgy, London (1980).
- Jaeger J.C., and Cook N.G.W.: *Fundamentals of rock Mechanics*, 3d edit.; Chapman and Hall (1979), 593 p.
- Jones R.H., Beauce A., Jupe A., Fabriol H., and Dyer B.C.: Imaging induced microseismicity during the 1993 injection tests at Soultz-sous-Forêts. *Proc. World Geotherm. Congr.*, Florence Inter. Geoth.l Ass., (1995), 2665–2669.
- Portier S, Vuataz F.D., Nami P., Sanjuan B., and Gérard A.: Chemical stimulation techniques for Geothermal wells: Experiments on the three wells EGS system at Soultz-sous-forêts (France), *Geothermics* **38**(4), (2009), 349-359.
- Schill E., Genter A., Cuenot N., and Kohl T.: Hydraulic performance history at the Soultz EGS reservoirs from stimulation and long-term circulation tests; *Geothermics*; **70**, (2017), 110-124
- Scholz, C. H.: *The Mechanics of Earthquakes and Faulting*, Cambridge University press (1990), 439 p.
- Shapiro, S.A., Audigane P., and Royer J.J.: Large-scale in situ permeability tensor of rocks from induced microseismicity, *Geophys. J. Int.*, **137**, (1999); 207–213
- Stein, S. and Wysession, M.: *An Introduction to Seismology, Earthquakes, and Earth Structure*, Blackwell publishing (2003), 498 p.
- Talebi S., and Cornet F.H.: Analysis of the microseismicity induced by fluid injection in a granitic rock mass, *Geophys. Res. Let.*, **14**(3), (1987), 227-230.
- Villeneuve M.C., Heap M.J., Kushnir A.R.L., Qin T., Beaud P., Zhou G., and Xu T.: Estimating in situ rock mass strength and elastic modulus of granite from the Soultz-sous-forêts geothermal reservoir (France), *Geothermal Energy*, 6(11), (2018), <https://doi.org/10.1186/s40517-018-0096-1>
- Yin J.M., and Cornet F.H.: Integrated stress determination by joint inversion of hydraulic tests and focal mechanisms, *Geophys. Res. Let.*, **21**(24), (1994), 2645-2648.